BIOCHEMISTRY
including biophysical chemistry & molecular biology

Article

pubs.acs.org/biochemistry

A Novel Assay for Detecting Fusion Pore Formation: Implications for the Fusion Mechanism

Hirak Chakraborty,[†] Pradip K. Tarafdar, and Barry R. Lentz*

Department of Biochemistry and Biophysics and Program in Molecular and Cellular Biophysics, University of North Carolina at Chapel Hill, Chapel Hill, North Carolina 27599-7260, United States

ABSTRACT: Membrane fusion is broadly envisioned as a two- or three-step process proceeding from contacting bilayers through one or two semistable, nonlamellar lipidic intermediate structures to a fusion pore. A true fusion event requires mixing of contents between compartments and is monitored by the movement of soluble molecules between trapped compartments. We have used poly(ethylene glycol) (PEG) to rapidly generate an ensemble aggregated state A that proceeds sequentially through intermediates (I_1 and/or I_2) to a final fusion pore state (FP) with rate constants k_1, k_2, and k_3. Movement of moderately sized solutes (e.g., Tb^{3+}/dipicolinic acid) has been used to detect pores assigned to intermediate states as well as to the final state (FP). Analysis of ensemble kinetic data has required that mixing of contents occurs with defined probabilities (α_i) in each ensemble state, although it is unclear whether pores that form in different states are different. We introduce here a simple new assay that employs fluorescence resonance energy transfer (FRET) between a 6-carboxyfluorescein (donor) and tetramethylrhodamine (acceptor), which are covalently attached to complementary sequences of 10 bp oligonucleotides. Complementary sequences of fluorophore-labeled oligonucleotides were incorporated in vesicles separately, and the level of FRET increased in a simple exponential fashion during PEG-mediated fusion. The resulting rate constant corresponded closely to the slow rate constant of FP formation (k_3) derived from small molecule assays. Additionally, the total extent of oligonucleotide mixing corresponded to the fraction of content mixing that occurred in state FP in the small molecule assay. The results show that both large "final pores" and small (presumably transient) pores can form between vesicles throughout the fusion process. The implications of this result for the mechanism of membrane fusion are discussed.

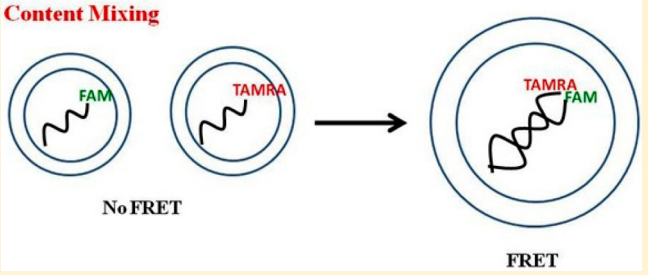

Membrane fusion is a ubiquitous event in eukaryotic cells, critical to organelle membrane trafficking, synaptic transmission, fertilization, enveloped viral infection, and myoblast syncytia formation. Nearly two decades of research has produced fairly wide agreement that membrane fusion proceeds in both model membranes and protein-laden biological membranes via the rearrangement of lipids[1,2] during a multistep process proceeding from contacting bilayers through one or two semistable, nonlamellar intermediate structures to a fusion pore, as envisioned in the "modified stalk hypothesis".[3,4] Because these structures form on a very small length scale (less than several nanometers) and evolve on a very fast time scale (several milliseconds[5]), it is not possible to test the modified stalk hypothesis by directly observing intermediate structures during single fusion events, although single-event measurements do confirm the existence of two or more steps in the process.[6,7] Distributions of average "wait times" between content mixing or lipid mixing single events (revealed by fluorescence methods)[8] show biexponential behavior, consistent with a process with at least two steps. Finally, analysis of ensemble kinetic measurements in terms of a two- or three-step model[9,10] yields rate constants comparable to the exponential constants derived from wait time distributions, which also supports the modified stalk hypothesis. While multiexponential behavior is detected by both ensemble kinetics and wait time analysis of single events, two studies, one using ensemble kinetics[11] and another analyzing wait time distributions of single events,[12] were able to resolve not just two exponentials but two processes with intervening lag phases, providing even more dramatic evidence of the modified stalk hypothesis.

Until recently,[7] both approaches (single-event and ensemble) failed to address whether pores between vesicles detected at different times during the fusion process (i.e., in different intermediate states) are similar or different. Early electrophysiological experiments on patch-clamped exocytic cells reported "flickering" or transient, small pores early in the fusion process.[13] This phenomenon was also reported in model membrane fusion[14] and was suggested by reports based on ensemble fusion kinetics,[11] although it is impossible to unambiguously detect transient or reversible pores using fluorescent probes, as pore opening results in an irreversible event, mainly rapid diffusion of fluorescent molecules between trapped compartments. It would clearly be useful to know whether pores formed early in the fusion process as monitored by ensemble kinetics are smaller than pores formed near the

Received: October 4, 2013
Revised: October 23, 2013
Published: October 28, 2013

end of the process, as might be implied by flickering pore observations. Here we introduce a new class of content mixing probe (fluorescently labeled 10 bp oligonucleotides) that monitor content mixing only through large pores. Measuring content mixing using these new oligo probes in combination with small molecule (Tb^{3+}/DPA) probes allowed us to parse for the first time by our ensemble kinetic methods the coexistence of two classes of pores throughout the fusion process.

MATERIALS AND METHODS

Materials. Chloroform stock solutions of 1,2-dioleoyl-3-*sn*-phosphatidylcholine (DOPC), 1,2-dioleoyl-3-*sn*-phosphatidylethanolamine (DOPE), 1,2-dioleoyl-3-*sn*-phosphatidylserine (DOPS), and bovine sphingomyelin (SM) were purchased from Avanti Polar Lipids (Birmingham, AL) and used without further purification. The concentration of the stock lipids was determined by a phosphate assay. Cholesterol (CH) was purchased from Avanti Polar Lipids and was further purified by published procedures.[15] Fluorescence-labeled oligonucleotides (5-FAM/TGGAGAAGGC and GCCTTCTCCA/3-TAMRA) were purchased from Integrated DNA Technologies. Poly(ethylene glycol) with a molecular weight of 7000−9000 (PEG 8000) was purchased from Thermo Fisher Scientific (Waltham, MA) and purified as previously reported.[16] All other reagents were of the highest purity available.

Vesicle Preparation. Vesicles were prepared from either a 35/30/15/20 DOPC/DOPE/SM/CH or a 32/25/15/20/8 DOPC/DOPE/SM/CH/DOPS molar mixture. Lipids at this molar ratio in a cyclohexane/methanol mixed solvent were freeze-dried under high vacuum overnight. The dried lipid powders were hydrated at 23 °C for 1 h in a sonication buffer that contained 10 mM TES, 100 mM NaCl, 1 mM EDTA, and 1 mM $CaCl_2$ (pH 7.4). Then small unilamellar vesicles were prepared using probe sonication as documented previously.[17] All content mixing, leakage, and lipid mixing experiments were performed at 0.2 mM lipid.

Preparation of Vesicles Containing the gp41 Fusion Peptide and Synaptobrevin Transmembrane Domain (TMD) Peptide. The gp41 fusion peptide from HIV (AVGIGALFLGFLGAAGSTMGARS) was chemically synthesized and purified by the peptide synthesis laboratory at the University of North Carolina at Chapel Hill. The peptide was synthesized by the standard solid phase method using Fmoc chemistry.[18,19] The transmembrane domain of synaptobrevin (SB-TMD) (KLKRKYWWKNLKMMIILGVICAIILIIIIVYFST) was purchased from Invitrogen and used without further purification. The purity of all the peptides was checked via mass spectrometry. For the gp41 fusion peptide, stock peptide solutions were prepared in DMSO and small aliquots of these solutions were added to vesicle suspensions at a peptide/lipid ratio of 1/200. DMSO was always less than 1% of the buffer volume, and control experiments showed that this amount of DMSO had no detectable effect on either fusion or membrane structure. For SB-TMD, the peptide was added to the chloroform solution of lipids at a peptide/lipid ratio of 1/900 and colyophilized with the lipids.

Initiation of the Fusion Reaction. The fusion process was initiated by adding 5 wt % PEG (with or without gp41 fusion peptide) for PC/PE/SM/CH small unilamellar vesicles (SUVs) and 6 wt % PEG for phosphatidylserine (PS)-containing SUVs. Signals were recorded within 6 s of the addition of PEG, such that vesicle aggregation was completed well before fusion events were recorded.

Lipid Mixing Assay. Fluorescent lipid probes with fluorophores attached to their acyl chains, BODIPY500-PC and BODIPY530-PE (Molecular Probes, Eugene, OR), were used for measuring lipid transfer during PEG- mediated vesicle fusion, with a probe-containing vesicle/probe-free vesicle ratio of 1/4, as described in detail elsewhere.[20,21] The ratio of labeled to unlabeled lipids in the probe-containing vesicles is 1/200. Here we normalized the F_D/F_A fluorescence intensity with respect to the F_D/F_A in the presence of the detergent, ideally a situation in which all lipids are mixed. In this method, the fraction of lipid mixing is

$$\mathrm{LM}(t) = \frac{1}{n}\exp\left\{\frac{k[(F_D/F_{DA})_t - (F_D/F_{DA})_0]}{(F_D/F_{DA})_{\mathrm{detergent}}} - 1\right\}$$

where n is the ratio of probe-free vesicles to probe-containing vesicles in a sample, F_D is the fluorescence of donor taken at a wavelength (520 nm) at which the acceptor does not contribute, F_A is the fluorescence of the acceptor taken at 560 nm (where there is little contribution from the donor), F_{DA} is the fluorescence of the donor in presence of the acceptor, and k is a calibration constant obtained for each experimental system (for SUVs fusing with SUVs, it ranges between 3.5 and 3.8). This somewhat unconventional quantity is related to but not equal to FRET efficiency but is ideally adapted to measurements in real time on a T-format fluorometer.[21]

Tb^{3+}/DPA Content Mixing and Leakage Assays. Mixing and leakage of the trapped contents of SUVs were monitored by the Tb^{3+}/DPA assay.[15] Vesicles were prepared in sonication buffer containing either 8 mM Tb^{3+} or 80 mM DPA and used in a 1/1 ratio in content mixing experiments. PEG was added as noted to trigger fusion, which was then monitored over time at 23 °C. Formation of a Tb^{3+}−DPA complex protects Tb^{3+} from quenching by water, producing an increase in fluorescence intensity. Content leakage was detected using vesicles containing co-encapsulated Tb^{3+} and DPA at concentrations of 4 and 40 mM, respectively, and measuring the loss of fluorescence over time.[15] All experiments were conducted at pH 7.4.

Fluorophore-Labeled Oligonucleotide-Based Content Mixing and Leakage Assay. 6-Carboxyfluorescein (FAM) and tetramethylrhodamine (TAMRA) are a classic example of a FRET pair, where FAM is the donor and TAMRA is the acceptor. The absorption maximum of FAM (donor) is 494 nm with an emission peak at 518 nm. TAMRA (acceptor) absorbs light emitted by FAM and emits at 580 nm. In our assay, FAM and TAMRA are tethered at the 5′ or 3′ ends of two 10-mer complementary sequences of oligonucleotides (Figure 1). SUVs were prepared in buffers containing either 5 μM FAM-oligonucleotide or 5 μM TMARA-oligonucleotides, with excess oligonucleotide probes removed using a Sephadex G-75 column. Membrane fusion was initiated as described by either 5 or 6 wt % PEG in a mixture of 100 μM (total lipid) TAMRA SUVs and 100 μM FAM SUVs. As large fusion pores form, fluorophore-labeled oligos move from one compartment to the other and the complementary oligos hybridize to bring the FRET pairs into the proximity of each other, producing an increase in FRET efficiency ($1 - F_{DA}/F_D$), or quenching of the donor fluorescence. Thus, the measurement of FRET efficiency as a function of time represents the kinetics of large fusion pore formation. This overall process required recording of two time

dx.doi.org/10.1021/bi401369j | *Biochemistry* 2013, 52, 8510−8517

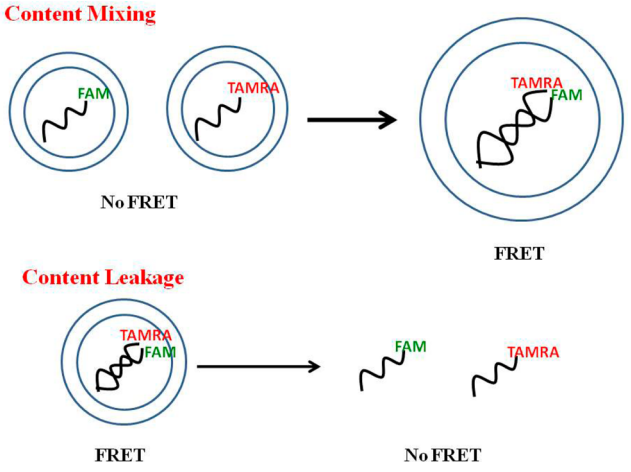

Figure 1. Illustration of the fluorescence-labeled oligonucleotide-based content mixing and leakage assays. Fluorescently labeled oligos 5-FAM/TGGAGAAGGC and GCCTTCTCCA/3-TAMRA were used to detect the content mixing and leakage. Oligo probes move from one membrane to other only through the expanded pore, which leads to hybridization of the oligonucleotide. 6-Carboxyfluorescein (FAM, donor) comes into close contact with tetramethylrhodamine (TAMRA, acceptor), leading to FRET.

courses. In the first, we monitored donor (FAM) fluorescence intensity (at 518 nm) in a mixture of 100 μM (lipid concentration) FAM-oligo-containing vesicles and 100 μM (lipid concentration) vesicles containing no fluorophore, with fusion triggered by PEG; this provides time course of F_D. In the second, we monitored donor fluorescence intensity (at 518 nm) when 100 μM FAM (donor)-oligo-containing vesicles were triggered to fuse with 100 μM TAMRA (acceptor)-oligo-containing vesicles using 5 or 6 wt % PEG; this provided the time course of F_{DA}. The time course of FRET efficiency ($1 - F_D/F_{DA}$) increase is the time course of large pore formation.

For content leakage experiments, 5 μM FAM- and 5 μM TMARA-containing oligonucleotides were co-encapsulated in SUVs; excess probes in external buffer were removed using a Sephadex G-75 column, and the loss of FRET was measured. Inside the vesicles, all the complementary strands are hybridized, and we observed maximal FRET. When vesicles were disrupted with detergent ($C_{12}E_8$), the FRET efficiency dropped precipitously because the concentrations of oligonucleotide in the external buffer were then less than femtomolar, which is much lower than the binding K_d of the two complementary sequences of 10-mer oligos. Note that the probe pair characterization shown in Figure 2 was performed at probe concentrations above the pair's K_d.

Data Analysis. We analyzed Tb^{3+}/DPA content mixing and leakage along with BODIPY500-PC and BODIPY530-PE lipid mixing data in terms of a sequential, three-state (two-step) fusion process (see the following diagram as described in detail previously[10]). Each "state" represents a thermodynamic ensemble of similar molecular arrangements ("microstructures"),[9] each of which is related to the structures proposed by Siegel and others,[3] although it is envisioned that the range of molecular microstructures contributing to each thermodynamic state is quite broad. Although they are not permitted by the structural model of Siegel, our data require that there are non-zero probabilities of content mixing (α) and lipid mixing (β) throughout the time evolution of the ensemble, consistent with the proposal that each state represents a multitude of different

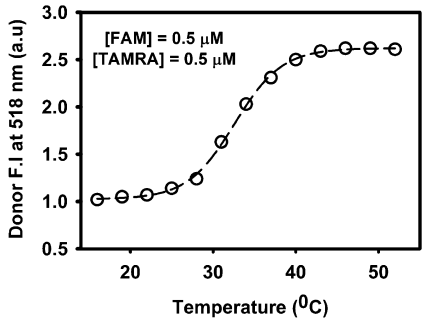

Figure 2. Melting profile of the complementary oligomers designed for the content mixing and leakage assay. At low temperatures, an equimolar (0.5 μM, above the K_d of the hybridized oligomeric complex) mixture of 5-FAM/TGGAGAAGGC (donor) and GCCT-TCTCCA/3-TAMRA (acceptor) hybridize and donor fluorescence is quenched due to FRET. The oligo duplex breaks down with an increase in temperature, and donor fluorescence increases. These data demonstrate that the designed pair of oligonucleotides will be a useful probe pair up to 30 °C.

microstructures, some of which would be expected to contain reversible or flickering pores[13] between trapped compartments. The ensemble kinetic model is illustrated by the following diagram

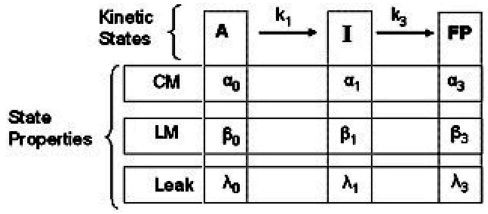

where A represents vesicles in contact within aggregates, I is the semistable intermediate state, and FP is the final fusion pore state (FP). The rate constants for conversion between ensemble states are k_1 for the A → I_1 step, k_2 for the I_1 → I_2 step, and k_3 for the I_2 → FP step.[9] For the particular system examined here, only a single intermediate is detected. Because fusion is likely to occur from the I_2 geometry, we assumed that I_1 and I_2 are rapidly interchangeable in these instances[22] and show a single intermediate, I (see diagram).

The model can account for the time courses of five observables associated with PEG-mediated fusion,[9] although the time courses of three basic observables, lipid mixing (LM), content mixing (CM), and leakage (L), are sufficient to uniquely define rate constants that account for the other two observables (light scattering, and formation and disappearance of nonlamellar intermediates[23]).[9,10,20] In addition to rate constants, the β_i and α_i values are probabilities and λ_i values are leakage rates required to describe the contribution of each state to particular observables (lipid mixing, content mixing, and content leakage). While this might seem to be an excessive number of parameters, experimental observations allow for elimination of some of these. The probabilities of content and lipid mixing in the A state were negligibly small (i.e., $\alpha_0 = \beta_0 = 0$), and a very small amount of lipid mixing takes place in the FP state (β_3 is assumed to be close to zero). Along with normalization conditions for the probabilities, this leads to two intrinsic rate constants (k_1 and k_3) and just five extensive parameters (α_1, β_1, λ_0, λ_1, and λ_3) to describe three independent time courses that in most cases are represented by double exponentials. A useful feature of this method is that the

dx.doi.org/10.1021/bi401369j | Biochemistry 2013, 52, 8510−8517

transitions are between thermodynamic states, so the temperature dependence of ensemble rate constants can yield the activation thermodynamics of each step.

RESULTS

Probe Pair Characterization. Because of the cooperative nature of oligonucleotide dimerization, it is critical to design an oligonucleotide FRET pair to match exactly the details of the planned experiment. We designed the oligonucleotide sequence for our probe pair using OligoAnalyze version 3.1 (Integrated DNA Technologies), so that the individual oligonucleotide strands did not form hairpin structures and did not undergo homodimerization at experimental temperatures. We also confirmed that the melting temperature of the oligonucleotide duplex is higher than our experimental temperature (23 °C). Figure 2 shows the donor (FAM) fluorescence intensity in a mixture of oligos at 0.5 μM each, as a function of temperature. The melting temperature (T_m) for the pair is ~33 °C, but at 23 °C, where we have performed our fusion experiments, the oligonucleotide pair was nearly all involved in forming a duplex that quenched donor fluorescence via FRET and increased FRET efficiency. A similar method using a 22-residue oligonucleotide was recently proposed and applied to single-event measurements in a model synaptic vesicle fusion process.[7,24] The difference between these two assays is that ours relies on the designed formation of the internucleotide hybrid at 23 °C to trigger an increase in FRET efficiency, while the other relies on designed loss of intra-oligonucleotide pairing (as triggered by a lipid-linked oligo in one vesicle population), resulting in a loss of FRET efficiency.[24]

Comparison of the Formation of Small and Large Pores in Four Model Membrane Systems. PEG-mediated model membrane fusion has been extensively used to examine the molecular mechanism of membrane fusion.[25] Here we test the applicability of this assay to four model membrane systems. Appropriate controls have already demonstrated that the low concentration of PEG used (5 or 6 wt %) does not alter bilayer or peptide structure[19] (P. K. Tarafdar and B. R. Lentz, unpublished observations).

Figure 3A shows the time course of content mixing between DOPC/DOPE/SM/CH (35/30/15/20) SUVs using the oligonucleotide-based assay at pH 7.4 in the absence and presence of gp41 fusion peptide (FP) at 23 °C and at a lipid:peptide ratio of 200:1. These conditions are optimal for observing the influence of the gp41 fusion peptide on fusion (H. Chakraborty, B. R. Lentz, et al., personal communication). This peptide promotes the rate of pore formation and increases the probability of content mixing earlier in the fusion process, as reflected by an increasing α_1 (Table 1). Panel ii of Figure 3B shows similar time courses using the common Tb^{3+}/DPA probe pair, while panels i and iii of Figure 3B show lipid mixing and content leakage time courses, respectively, for this vesicle system. We measured leakage of the oligo probes by encapsulating both the probes in one set of vesicles and then following the time course of loss of FRET efficiency (see Materials and Methods). We detected no more than 1.5% leakage for any of the systems described here (data not shown). It is immediately obvious from Figure 3A and panel ii of Figure 3B that these two types of assays for content mixing report very different events occurring on different time scales. The three time courses recorded in panels i–iii of Figure 3B all required description by double-exponential curves but together allowed us to analyze the data obtained with the Tb^{3+}/DPA content

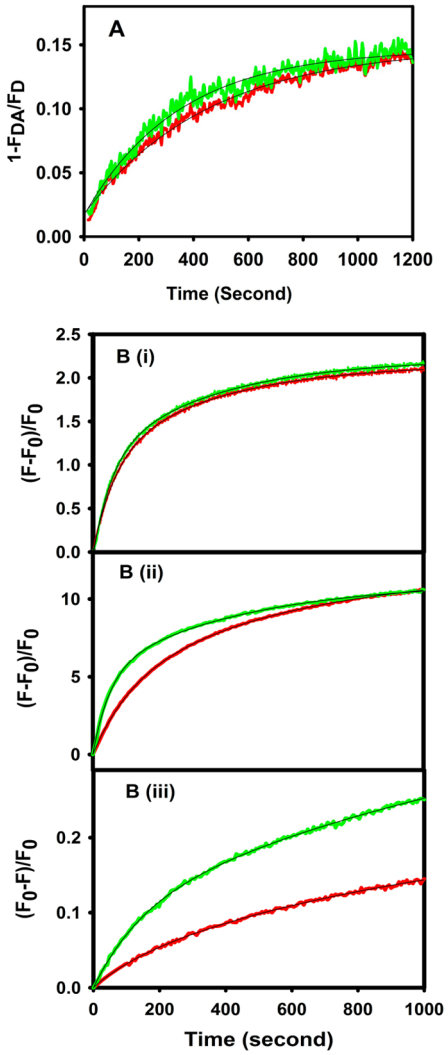

Figure 3. Comparison of time courses of content mixing using the oligonucleotide-based assay and small molecule-based assay for vesicles with and without the HIV gp41 fusion peptide. (A) Content mixing was conducted for DOPC/DOPE/SM/CH (35/30/15/20) SUVs at pH 7.4 in the absence (red) and presence (green) of the gp41 fusion peptide in a peptide:lipid ratio of 1:200 using the oligonucleotide-based assay. The time course was best described by single-exponential equation $y = y_0 + a(1 - e^{-bx})$, with the resulting parameters listed in Table 1. (B) Traces of (i) lipid mixing, (ii) content mixing, and (iii) content leakage for the PC/PE/SM/CH SUVs at pH 7.4 using conventional assays[10] in the absence (red) and presence (green) of the gp41 fusion peptide at a peptide:lipid ratio of 1:200. Membrane fusion was induced with 5% PEG at 23 °C. F is the fluorescence intensity at time t, and F_0 is the fluorescence intensity at time zero. Measurements were taken in 10 mM MES, 100 mM NaCl, 1 mM $CaCl_2$, and 1 mM EDTA (pH 5.0) at a total lipid concentration of 0.2 mM. The smooth curves drawn through the data represent three-state sequential model global fits.

mixing and leakage assay in terms of our ensemble kinetic treatment as described in Materials and Methods.[9,10] This treatment determines a rate constant k_1 for converting the aggregated state (A) to the initial intermediate state (I), which then converts to a final fusion pore (FP state) with rate constant k_3.[9,10,22] These rate constants along with other parameters defined by the ensemble kinetics analysis, α_1 (probability of content mixing in state I) and f_{CM} (total extent of content mixing), are listed in Table 1. By contrast, the time

dx.doi.org/10.1021/bi401369j | Biochemistry 2013, 52, 8510–8517

Table 1. Summary of the Analysis of LM, CM, and Leakage Experiments in the Absence and Presence of the Peptide using a Three-State Sequential Model[a]

system (peptide/lipid)	k_1 ($\times 10^3$)	k_3 ($\times 10^3$)	α_1	α_3	f_{CM}	$\alpha_3 f_{CM}$	k_O ($\times 10^3$) from the oligo assay	$f_{CM,O}$ from the oligo assay
PC/PE/SM/CH	16.0 ± 0.5	1.69 ± 0.01	0.28 ± 0.010	0.72 ± 0.1	0.25 ± 0.2	0.18 ± 0.04	1.90 ± 0.04	0.14 ± 0.04
gp41 FP (1/200) in PC/PE/SM/CH	18.0 ± 0.22	1.86 ± 0.04	0.44 ± 0.02	0.56 ± 0.02	0.27 ± 0.03	0.15 ± 0.02	2.3 ± 0.05	0.15 ± 0.03
PC/PE/SM/CH/PS	5.78 ± 0.31	0.53 ± 0.08	0.25 ± 0.01	0.75	0.15 ± 0.2	0.11 ± 0.01	0.42 ± 0.02	0.12 ± 0.03
SB-TMD (1/900) in PC/PE/SM/CH/PS	8.83 ± 0.47	0.98 ± 0.09	0.34 ± 0.01	0.66	0.16 ± 0.03	0.11 ± 0.03	1.56 ± 0.02	0.12 ± 0.03

[a]Also included are the rates of pore formation and the extents of content mixing using the oligonucleotide-based assay. Experiments were conducted 23 °C and at pH 7.4. k_1 and k_2 are rate constants of intermediate and final pore formation, respectively. α_1 and α_3 are the probabilities of content mixing (in the Tb/DPA assay) in the intermediate and final pore states, respectively. f_{CM} is the total (as a fraction of possible) content mixing. $\alpha_3 f_{CM}$ is the total content mixing through the final pore using the Tb/DPA assay. k_O is the rate constant of pore formation using the oligonucleotide-based assay. $f_{CM,O}$ is the total (as a fraction of possible) content mixing using the oligonucleotide-based assay.

courses in Figure 3A were appropriately described by a single-exponential equation (rate constant k_O) and thus likely represent a single kinetic process. The extent of total possible oligonucleotide content mixing ($f_{CM,O}$; see Table 1 legend) was determined using vesicles containing co-encapsulated FAM and TAMRA oligonucleotides. Parameters k_O and $f_{CM,O}$ for PEG-mediated fusion of PC/PE/SM/CH SUVs are listed in Table 1. The rate of oligonucleotide movement between compartments [i.e., the rate of large pore formation; $k_O = (1.9 \pm 0.04) \times 10^{-3}$ s^{-1}] was quite similar to the rate, k_3 [$(1.7 \pm 0.01) \times 10^{-3}$ s^{-1}], of final pore formation obtained using the Tb^{3+}/DPA content mixing assay. In addition, the amount of total Tb^{3+}/DPA content mixing occurring in the FP (final pore) state ($\alpha_3 f_{CM}$ = 0.18 ± 0.04) was also similar to the amount of total content mixing ($f_{CM,O}$) obtained from the oligonucleotide assay (0.14 ± 0.04). These similarities suggest that formation of state FP (final fusion pore) is related to the formation of large pores detected by oligonucleotides.

The kinetics and activation thermodynamics of PEG-mediated fusion vary considerably with the lipid composition of SUVs.[9,10,22,26] To test whether the results in the first row of Table 1 might be specific to a given lipid composition, we examined PEG-mediated fusion of DOPC/DOPE/SM/CH/DOPS (32/25/15/20/8) SUVs. The presence of DOPS alters fusion behavior significantly.[26] Row 3 of Table 1 summarizes the results of these experiments. Again, we note the close correspondence of k_3 [$(0.53 \pm 0.08) \times 10^{-3}$ s^{-1}] to k_O [$(0.42 \pm 0.02) \times 10^{-3}$ s^{-1}] as well as the similarity of $\alpha_3 f_{CM}$ (0.11 ± 0.01) to $f_{CM,O}$ (0.12 ± 0.03), strongly supporting the hypothesis that the formation of FP corresponds to the formation of large pores. Phosphatidylserine (PS) is required for the observation of the catalytic influence of the transmembrane domain of the SNARE protein synaptobrevin (P. K. Tarafdar, B. R. Lentz, et al., personal communications). In PS-containing membranes, it enhances both the rates of initial intermediate and final pore formation and the probability of pore formation early in the fusion process, α_1 (Table 1).

Results from experiments with both catalytic peptides examined, as incorporated into their two optimal SUV compositions, showed they increased both k_3 from the Tb^{3+}/DPA assay and k_O from the oligonucleotide assay to roughly the same extent (Figure 4).

DISCUSSION

Pore Formation Assays. While it would seem to be obvious that oligonucleotides should be useful for following large pore formation during fusion, we knew of only one paper that has taken this approach when we started this work.[27] This work used radioactive nucleotides, so it was not very useful in following rates of content mixing. The use of fluorescently labeled oligonucleotides as "molecular beacons" to detect oligo sequences was suggested in 1966.[28] A very recent paper used the molecular beacon concept to detect large pore formation by chemically linking oligonucleotides to lipids in target vesicles.[7] The work presented here introduces a unique probe that allows continuous monitoring of content mixing via FRET but without requiring oligonucleotides chemically linked to lipids. We estimated the size of the probe to be ~2 nm in rotational diameter when it was unfolded.[29] A folded 22-residue stem–loop oligonucleotide probe is similarly estimated to be ~2 nm in diameter by MD simulations.[7] Tb^{3+} has an ionic radius of 1.2 Å but is also likely to have a hydration shell of perhaps 1 Å, leaving it with a hydrated diameter of ~4–5 Å. The chemical structure of dipicolinic acid suggests that it should have a rotational diameter of 6–8 Å. Thus, both Tb^{3+} and DPA are very small molecules capable of passing through pores that are roughly ~5 times smaller than those available to oligonucleotide probes.

Two Classes of Pores. Estimates of the size of fusion pores vary widely. Electron micrographs can resolve continuities between synaptic vesicles and synaptic space of ~5–10 nm in diameter.[30] However, conductance and capacitance measurements during secretory vesicle release suggest that initial pores open very quickly (≲1 ms) and are very small (≲1 nm[31]). It is also clear that these initially very small pores can reclose or expand to form much larger pores (5–10 nm).[31] A consequence of this appears to be observation of flickering pores during mast cell granule and chromaffin cell release that precede final release.[13,32] Flickering pores have also been reported to form during osmotically triggered fusion of vesicles with black lipid membranes.[14] The existence of very small (capable of passing H^+ only) pores early in PEG-mediated fusion of very "nonleaky" 45 nm dilinolenoylPC/DOPC (15/85) vesicles has been reported.[11] Finally, the correlation of leakage rate to the probability of fusion in intermediate (I_1 or I_2) versus FP states previously was suggested to support two classes of pores during PEG-mediated fusion: early pores associated with leakage and later pores less correlated with leakage.[9] Schick and co-workers[33] proposed, on the basis of coarse-grain Monte Carlo simulations, that both leakage and intervesicle pores are associated with "stalk" structures (I state) presumed to exist very early in the fusion process but then growing to larger structures.

dx.doi.org/10.1021/bi401369j | Biochemistry 2013, 52, 8510–8517

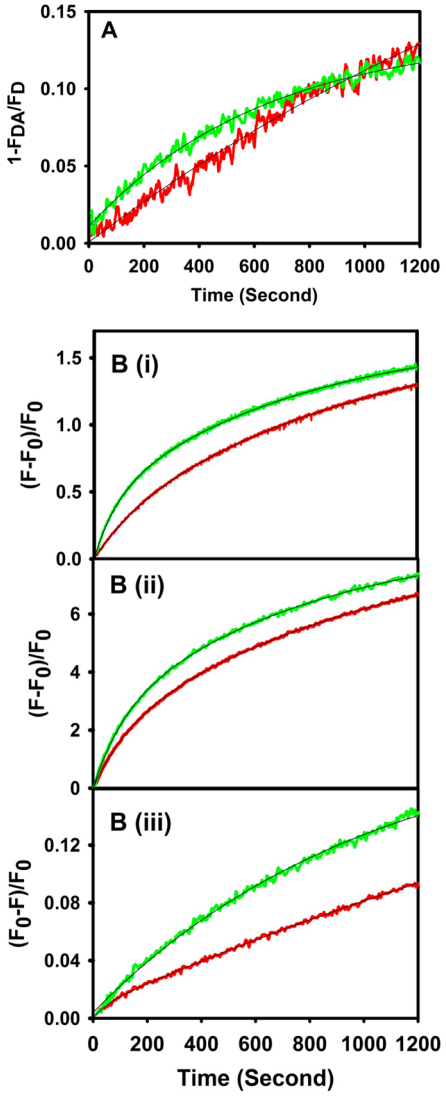

Figure 4. Comparison of time courses of content mixing using the oligonucleotide-based assay and small molecule-based assay for vesicles with and without the synaptobrevin transmembrane domain peptide. (A) Content mixing was conducted for DOPC/DOPE/SM/CH/DOPS (32/25/15/20/8) SUVs at pH 7.4 in the absence (red) and presence (green) of the synaptobrevin transmembrane domain at a peptide:lipid ratio of 1:900 using the oligonucleotide-based assay. The time course was best described by single-exponential equation $y = y_0 + a(1 - e^{-bx})$, with the resulting parameters listed in Table 1. (B) Traces of (i) lipid mixing, (ii) content mixing, and (iii) content leakage for the PC/PE/SM/CH SUVs at pH 7.4 in the absence (red) and presence (green) of the synaptobrevin transmembrane domain (green) at a peptide:lipid ratio of 1:900 using the small molecule-based assay. For all cases, membrane fusion was induced by 6% PEG at 23 °C. Measurements were taken in 10 mM MES, 100 mM NaCl, 1 mM $CaCl_2$, and 1 mM EDTA at a total lipid concentration of 0.2 mM. The smooth curves drawn through the data represent three-state sequential model global fits.

The results reported here are consistent with the existence of early transient pores and later larger pores and offer a more precise definition of "final pores" that form during PEG-mediated fusion. Of course, results supporting two pore sizes cannot show that the smaller pores are flickering or transient, although this is consistent with the electrical and other measurements discussed above. The results summarized in Table 1 strongly support the hypothesis that final pores are equivalent to the large pores defined by oligonucleotide mixing between SUVs, i.e., pores with diameters of ~2 nm. Because the diameter of an SUV is ~23−25 nm, it is unlikely that more than one such large pore could form between SUVs at one time and one point of contact. A pore of this size would require lipid rearrangements substantially larger than the correlated movements of only a few lipids that have been suggested to constitute the transition state to pore formation.[10] Such substantial lipid rearrangements are reported to occur at rates comparable to that of final pore formation. At the PEG threshold concentration for observing fusion, lipids redistribute from outer to inner leaflets of 15/85 dilinolenoylPC/DOPC SUVs at a slow rate of $\sim 4.6 \times 10^{-3}$ s^{-1}, which is comparable to that of inner-leaflet lipid mixing ($\sim 3.7 \times 10^{-3}$ s^{-1}) or content mixing ($\sim 5.8 \times 10^{-3}$ s^{-1}) for this system.[34] This paper also reported that the polarity at the methylamine of TMA-DPH (trimethylamine diphenylhexatriene) decreased exponentially at an even slower rate ($\sim 2 \times 10^{-3}$ s^{-1}),[34] implying that remnant curvature stress continued to slowly dissipate even after lipids redistributed sufficiently to form a large pore. With the results reported here, we suggest that slow content mixing events reported here correspond to formation of large final pores and that this predictably requires transbilayer and other lipid rearrangement. The faster content and lipid mixing rates can reasonably be assigned to transient pores, for which less dramatic lipid rearrangements should be required.

Membrane-contacting regions (transmembrane domains and "fusion peptides") of fusion proteins catalyze both steps of the fusion process in the two lipid systems examined and promote pore formation earlier in the process (H. Chakraborty, P. K. Tarafdar, B. R. Lentz, et al., personal communications), so the fact that both these membrane-contacting regions promote the rate of large pore formation as judged by both the oligonucleotide and the rate of final pore formation using a small-molecule content mixing assay (Table 1) is strong support for our conclusions. Interestingly, while both peptides increase α_1, they decrease α_3, so that the extent of content mixing that occurs though large pores ($\alpha_3 f_{CM} = f_{CM,O}$) remains unchanged (Table 1).

Large Pores Are Observed throughout the Fusion Process. A potentially surprising aspect of our results is that both final pores and small pores form throughout the fusion process. The sequential model of fusion posits that the initial aggregated state of closely contacting SUVs proceeds through intermediates to the final fusion pore state. In this picture, rate k_1 of intermediate formation corresponds to the rate of minor lipid rearrangements (lipid mixing) that lead to content leakage or content mixing pores.[33] If the intermediate forms prior to FP, we expect to see biexponential kinetics in which the two exponentials may or may not be clearly resolved depending on how similar k_1 and k_3 are.[9] We nearly always resolve one fast component (lipid mixing and transitory pore formation) and a 10-fold slower component [final large pore formation (see Table 1)]. In a recent single-event analysis of Ca^{2+}-triggered fusion between tethered vesicles, the distribution of dwell times for content mixing events was also reported to be a double exponential, with the slow exponential having a decay constant roughly 1 order of magnitude smaller than the fastest.[8] Thus, both ensemble kinetic and dwell time analyses of multiple single events support the coexistence of slow and fast content and lipid mixing components, with our current results attributing the slow component to the formation of large pores.

dx.doi.org/10.1021/bi401369j | Biochemistry 2013, 52, 8510−8517

A more recent dwell time analysis compared the movement of small molecules and DNA oligonucleotides between docked vesicles as stimulated by Ca^{2+} and synaptotagmin.[7] This study reported a very small amount of large pore formation, but unlike our ensemble results, the dwell time distribution was biphasic, with a very slow phase preceding a faster phase. As we point out, ensemble kinetic measurements and dwell time analyses of individual events should yield similar results, because they describe averages over many vesicle pairs and over many vesicle pair events, respectively. It is difficult to say with certainty the reason for the disagreement between our results and those of Lai et al.[7] One possibility could be that the greater time resolution of the dwell time analysis (200 ms) allows detection of the initial lag time. However, another recent dwell time analysis with a similar time resolution (200 or 500 ms) reported only two time constants, differing by roughly 1 order of magnitude, for Ca^{2+}-triggered content mixing between SNARE- and synaptotagmin-linked vesicles, an observation consistent with our ensemble kinetic measurements of PEG-triggered fusion.[8] Another possibility is that both Ca^{2+} and synaptotagmin were needed to complete molecular rearrangements of the syntaxin−v-SNARE complex,[7] so the slow process could correspond to completion of the appropriate closely contacted state required for fusion. The rate and extent of fusion vary with how closely vesicles are forced into contact,[35] so if this interbilayer distance changes as intervesicle complexes mature, this could cause a delay in the initiation of the fusion process. Finally, Lai et al. and we have studied very different systems, Ca^{2+}-triggered fusion of SNARE and synaptotagmin-linked 100 nm vesicles and PEG-triggered fusion of PEG-aggregated 23 nm SUVs, with both vesicle preparations having different compositions. A strong argument against this final possibile explanation is our observation that the phenomenon reported here ($k_3 \approx k_O$) holds for two very different lipid compositions and for SUVs in the presence or absence of membrane-contacting catalytic sequences from two types of fusion proteins. We conclude that it is likely that large pores appear throughout the fusion process at least as detected by ensemble kinetic analysis but likely also as detected by dwell time analysis of many independent fusion events.[8]

Is the Fusion Process Sequential As Proposed by the Modified Stalk Hypothesis? If the process is sequential, how is it that the FP state appears throughout the fusion process? The answer lies in the ensemble nature of our experiments and analysis[9,10,20,26] and in the similar ensemble nature of dwell time analysis of single events.[8] The modified stalk hypothesis,[3] as applied to fusion of a single pair of highly curved vesicles, predicts that the free energy of intermediate structures from the initial stalk (I_1) to the final prefusion intermediate (I_2) evolves continuously as the geometry and structure of the pair of hemifused vesicles evolve.[36] This is a sequential structural model. When translated to an ensemble model, there will be many different structural species of closely apposed SUV pairs in any intermediate ensemble state that contribute to the evolving ensemble process as well as to the transition states (TS) between semistable states. Analysis of ensemble kinetic experiments performed at different temperatures provides estimates of the activation thermodynamics of each step of the ensemble fusion process in which one ensemble state evolves to another.[10] According to this analysis, the transition state between intermediate I (the intermediate) and FP, which is termed TS3,[10,36] is very similar to the I state but differs in the average radii (termed "stalk radius") of single-bilayer diaphragms between the trapped compartments in the "hemifused" I state and transition state TS3. The circumference of this diaphragm is predicted to be quite unstable,[33,36] supporting the possibility that "correlated fluctuations" of multiple lipids in the diaphragm might account for the activation thermodynamics of pore formation.[10] We suggest that these fluctuations, being random events, can occur at any time during the evolution of I through TS3 to FP but should increase in number with increasing average stalk radius, which increases as the system approaches the FP state.[36] This ensemble kinetic model is thus consistent with our observation that both small and large pores can occur at any time during the process. However, the slow component of content mixing $[\alpha_3 \times FP(t)]$ is still growing long after the fast component largely levels out at early times. In this picture, every vesicle pair can evolve toward a large final fusion pore by a sequential structural mechanism according to the model of Siegel, while the entire ensemble can evolve such that large and small pores can occur at any time, but with large pores contributing increasingly to content mixing at long times. If k_1 and k_3 were sufficiently different, or if a sufficiently slow event separated these intermediate and pore formation events, it might be possible to resolve the sequential nature of the process from ensemble kinetics, as we have reported,[11] but in most instances, this is not the case.

■ SUMMARY

We introduce a new assay for the mixing of large solutes (oligonucleotides) between trapped fusion compartments and use this to demonstrate that large and small pores form throughout the fusion process, as detected by ensemble methods. The relevance of these results to single-event studies of membrane fusion is discussed, as is the relation of an ensemble model to a single-event structural model.

■ AUTHOR INFORMATION

Corresponding Author

*Department of Biochemistry and Biophysics and Program in Molecular and Cellular Biophysics, University of North Carolina at Chapel Hill, Chapel Hill, NC 27599. E-mail: uncbrl@med.unc.edu. Phone: (919) 966-5384.

Present Address

[†]H.C.: Centre for Cellular and Molecular Biology, Council of Scientific and Industrial Research, Hyderabad 500 007, India.

Funding

This work is supported by National Institutes of Health Grant GM32707 to B.R.L.

Notes

The authors declare no competing financial interest.

■ REFERENCES

(1) Chernomordik, L. V., and Kozlov, M. M. (2008) Mechanics of membrane fusion. *Nat. Struct. Mol. Biol. 15*, 675−683.

(2) Lee, J., and Lentz, B. R. (1998) Secretory and viral fusion may share mechanistic events with fusion between curved lipid bilayers. *Proc. Natl. Acad. Sci. U.S.A. 95*, 9274−9279.

(3) Siegel, D. P. (1999) The modified stalk mechanism of lamellar/inverted phase transitions and its implications for membrane fusion. *Biophys. J. 76*, 291−313.

(4) Kozlov, M. M., Leikin, S. L., Chernomordik, L. V., Markin, V. S., and Chizmadzhev, Y. A. (1989) Stalk mechanism of vesicle fusion. Intermixing of aqueous contents. *Eur. Biophys. J. 17*, 121−129.

(5) Oberhauser, A. F., Monck, J. R., and Fernandez, J. M. (1992) Events leading to the opening and closing of the exocytotic fusion pore have markedly different temperature dependencies. Kinetic analysis of single fusion events in patch-clamped mouse mast cells. *Biophys. J. 61*, 800−809.
(6) Yoon, T. Y., Okumus, B., Zhang, F., Shin, Y. K., and Ha, T. (2006) Multiple intermediates in SNARE-induced membrane fusion. *Proc. Natl. Acad. Sci. U.S.A. 103*, 19731−19736.
(7) Lai, Y., Diao, J., Liu, Y., Ishitsuka, Y., Su, Z., Schulten, K., Ha, T., and Shin, Y.-K. (2013) Fusion pore formation and expansion induced by Ca^{2+} and synaptotagmin 1. *Proc. Natl. Acad. Sci. U.S.A. 110*, 1333−1338.
(8) Kyoung, M., Srivastava, A., Zhang, Y., Diao, J., Vrljic, M., Grob, P., Nogales, E., Chu, S., and Brunger, A. T. (2011) In vitro system capable of differentiating fast Ca^{2+}-triggered content mixing from lipid exchange for mechanistic studies of neurotransmitter release. *Proc. Natl. Acad. Sci. U.S.A. 108*, 11737−11738.
(9) Weinreb, G., and Lentz, B. R. (2007) Analysis of membrane fusion as a two-state sequential process: Evaluation of the stalk model. *Biophys. J. 92*, 4012−4029.
(10) Chakraborty, H., Tarafdar, P. K., Bruno, M. J., Sengupta, T., and Lentz, B. R. (2012) Activation thermodynamics of poly(ethylene glycol)-mediated model membrane fusion support mechanistic models of stalk and pore formation. *Biophys. J. 102*, 2751−2760.
(11) Lee, J., and Lentz, B. R. (1997) Evolution of lipidic structures during model membrane fusion and the relation of this process to cell membrane fusion. *Biochemistry 36*, 6251−6259.
(12) Lee, H.-K., Yang, Y., Su, Z., Hyeon, C., Lee, T.-S., Lee, H.-W., Kweon, D.-H., Shin, Y.-K., and Yoon, T.-Y. (2010) Dynamic Ca^{2+}-dependent stimulation of vesicle fusion by membrane-anchored synaptotagmin 1. *Science 328*, 760−763.
(13) Alvarez de Toledo, G., Fernandez-Chacon, R., and Fernandez, J. M. (1993) Release of secretory products during transient vesicle fusion. *Nature 363*, 554−558.
(14) Chanturiya, A., Chernomordik, L. V., and Zimmerberg, J. (1997) Flickering fusion pores comparable with initial exocytotic pores occur in protein-free phospholipid bilayers. *Proc. Natl. Acad. Sci. U.S.A. 94*, 14423−14428.
(15) Haque, M. E., McIntosh, T. J., and Lentz, B. R. (2001) Influence of lipid composition on physical properties and peg-mediated fusion of curved and uncurved model membrane vesicles: "Nature's own" fusogenic lipid bilayer. *Biochemistry 40*, 4340−4348.
(16) Lentz, B. R., McIntyre, G. F., Parks, D. J., Yates, J. C., and Massenburg, D. (1992) Bilayer curvature and certain amphipaths promote poly(ethylene glycol)-induced fusion of dipalmitoylphosphatidylcholine unilamellar vesicles. *Biochemistry 31*, 2643−2653.
(17) Lentz, B. R., Carpenter, T. J., and Alford, D. R. (1987) Spontaneous fusion of phosphatidylcholine small unilamellar vesicles in the fluid phase. *Biochemistry 26*, 5389−5397.
(18) Haque, M. E., and Lentz, B. R. (2002) Influence of gp41 fusion peptide on the kinetics of poly(ethylene glycol)-mediated model membrane fusion. *Biochemistry 41*, 10866−10876.
(19) Haque, M. E., McCoy, A. J., Glenn, J., Lee, J., and Lentz, B. R. (2001) Effects of hemagglutinin fusion peptide on poly(ethylene glycol)-mediated fusion of phosphatidylcholine vesicles. *Biochemistry 40*, 14243−14251.
(20) Haque, M. E., Chakraborty, H., Koklic, T., Komatsu, H., Axelsen, P. H., and Lentz, B. R. (2011) Hemagglutinin fusion peptide mutants in model membranes: Structural properties, membrane physical properties, and PEG-mediated fusion. *Biophys. J. 101*, 1095−1104.
(21) Malinin, V. S., Haque, M. E., and Lentz, B. R. (2001) The rate of lipid transfer during fusion depends on the structure of fluorescent lipid probes: A new chain-labeled lipid transfer probe pair. *Biochemistry 40*, 8292−8299.
(22) Sengupta, T.; Chakraborty, H.; Lentz, B. R. The transmembrane domain peptide of Vesicular Stomatitis Virus promotes both intermediate and pore formation during PEG-mediated vesicle fusion. *Biophys. J.* 2013, (under revision).
(23) Malinin, V. S., and Lentz, B. R. (2002) Pyrene Cholesterol Reports the Transient Appearance of Nonlamellar Intermediate Structures during Fusion of Model Membranes. *Biochemistry 41*, 5913−5919.
(24) Diao, J., Ishitsuka, Y., Lee, H., Joo, C., Su, Z., Syed, S., Shin, Y. K., Yoon, T. Y., and Ha, T. (2012) A single vesicle-vesicle fusion assay for in vitro studies of SNAREs and accessory proteins. *Nat. Protoc. 7*, 921−934.
(25) Lentz, B. R. (2007) PEG as a tool to gain insight into membrane fusion. *Eur. Biophys. J. 36*, 315−326.
(26) Tarafdar, P. K., Chakraborty, H., Dennison, S. M., and Lentz, B. R. (2012) Phosphatidylserine inhibits and calcium promotes model membrane fusion. *Biophys. J. 103*, 1880−1889.
(27) Nickel, W., Weber, T., McNew, J. A., Parlati, F., Sollner, T. H., and Rothman, J. E. (1999) Content mixing and membrane integrity during membrane fusion driven by pairing of isolated v-SNAREs and t-SNAREs. *Proc. Natl. Acad. Sci. U.S.A. 96*, 12571−12576.
(28) Tyagi, S., and Kramer, F. R. (1996) Molecular beacons: Probes that fluoresce upon hybridization. *Nat. Biotechnol. 14*, 303−308.
(29) http://www.calctool.org/CALC/prof/bio/dna.
(30) Zampighi, G. A., Zampighi, L. M., Fain, N., Lanzavecchia, S., Simon, S. A., and Wright, E. M. (2006) Conical Electron Tomography of a Chemical Synapse: Vesicles Docked to the Active Zone are Hemi-Fused. *Biophys. J. 91*, 2910−2918.
(31) Spruce, A. E., Breckenridge, L. J., Lee, A. K., and Almers, W. (1990) Properties of the fusion pore that forms during exocytosis of a mast cell secretory vesicle. *Neuron 4*, 643−654.
(32) Chow, R. H., von Ruden, L., and Neher, E. (1992) Delay in vesicle fusion revealed by electrochemical monitoring of single secretory events in adrenal chromaffin cells. *Nature 356*, 60−63.
(33) Muller, M., Katsov, K., and Schick, M. (2003) A new mechanism of model membrane fusion determined from Monte Carlo simulation. *Biophys. J. 85*, 1611−1623.
(34) Evans, K. O., and Lentz, B. R. (2002) Kinetics of Lipid Rearrangements during Poly(ethylene glycol)-Mediated Fusion of Highly Curved Unilamellar Vesicles. *Biochemistry 41*, 1241−1249.
(35) Burgess, S. W., McIntosh, T. J., and Lentz, B. R. (1992) Modulation of poly(ethylene glycol)-induced fusion by membrane hydration: Importance of interbilayer separation. *Biochemistry 31*, 2653−2661.
(36) Malinin, V. S., and Lentz, B. R. (2004) Energetics of vesicle fusion intermediates: Comparison of calculations with observed effects of osmotic and curvature stresses. *Biophys. J. 86*, 2951−2964.